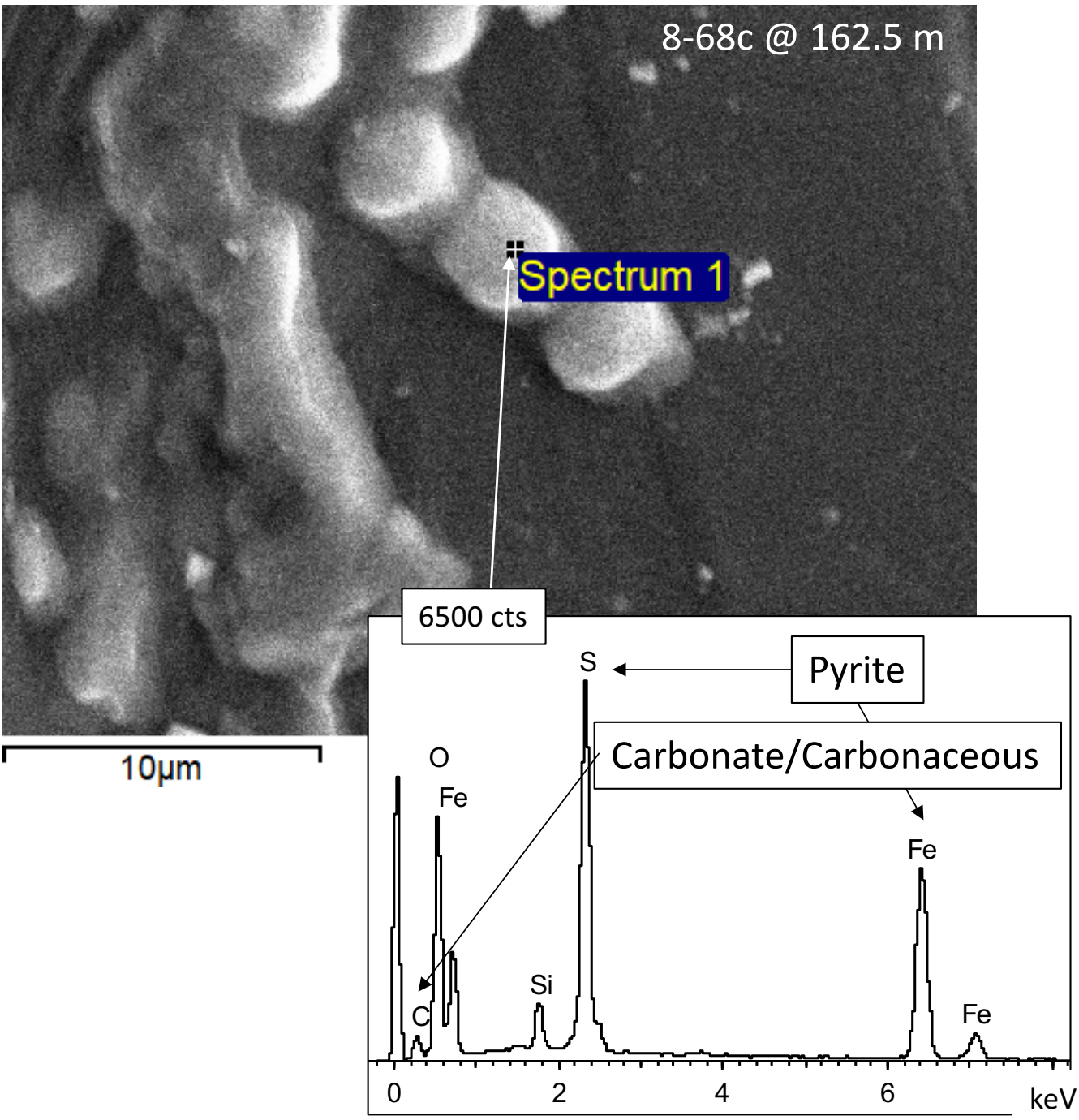

Supp. Fig. 1. Mucilaginous capsule-embedding spheroid rows found in sample 8-68c at a depth of 162.5 m.

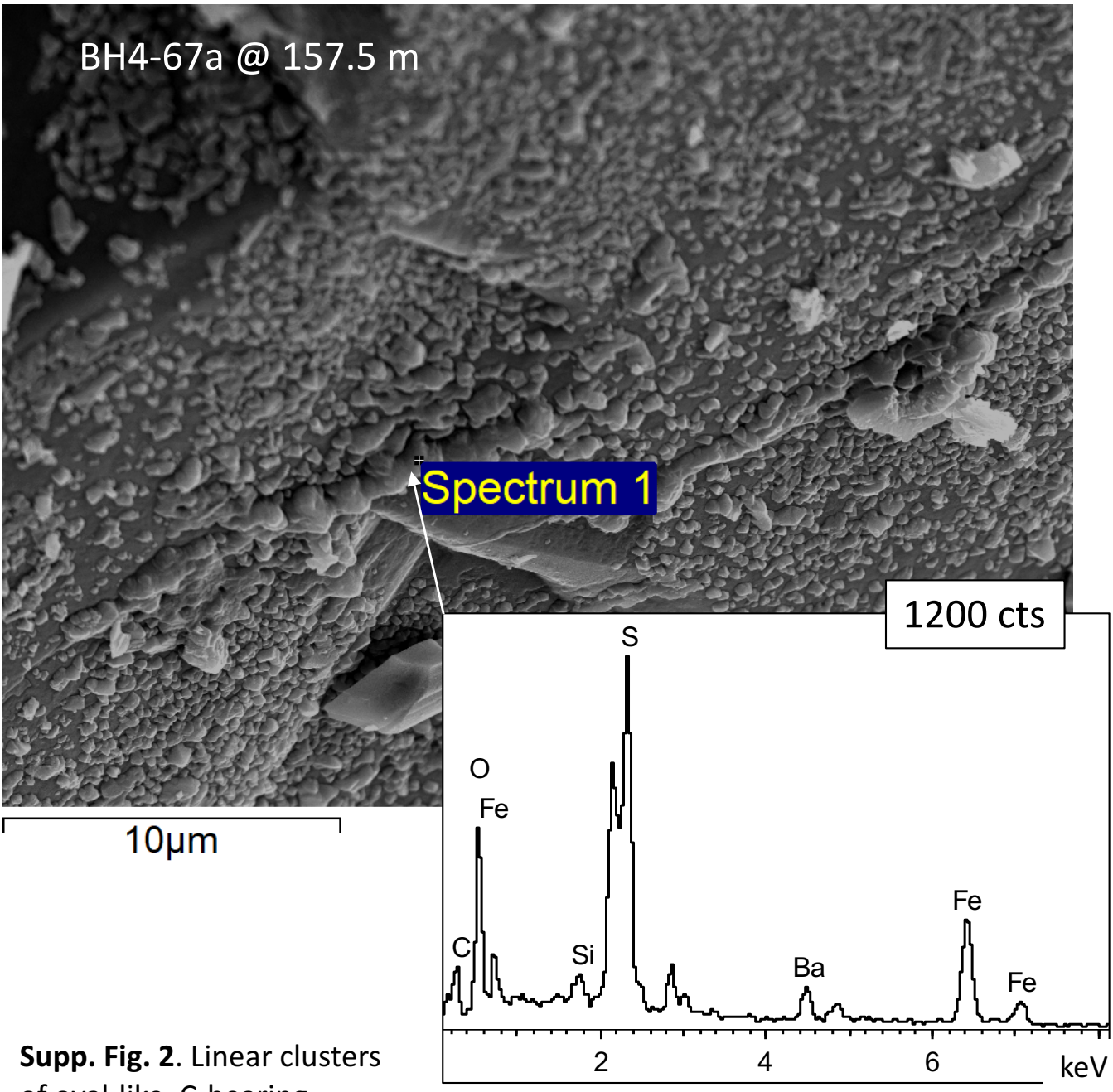

Supp. Fig. 2. Linear clusters of oval-like, C-bearing structures on a pyrite surface found in sample 4-67a that is shown in Fig. 3a and which EDAX spectrum suggest a Fe-carbonate composition..

Element	Weight%		Atomic%
C	2.26 +/-	0.32	38.81
O	2.87 +/-	0.14	37.00
Si	0.09 +/-	0.02	0.64
S	1.79 +/-	0.05	11.47
Fe	2.84 +/-	0.10	10.49
Ba	1.06 +/-	0.08	1.59
Totals	10.92		100.00

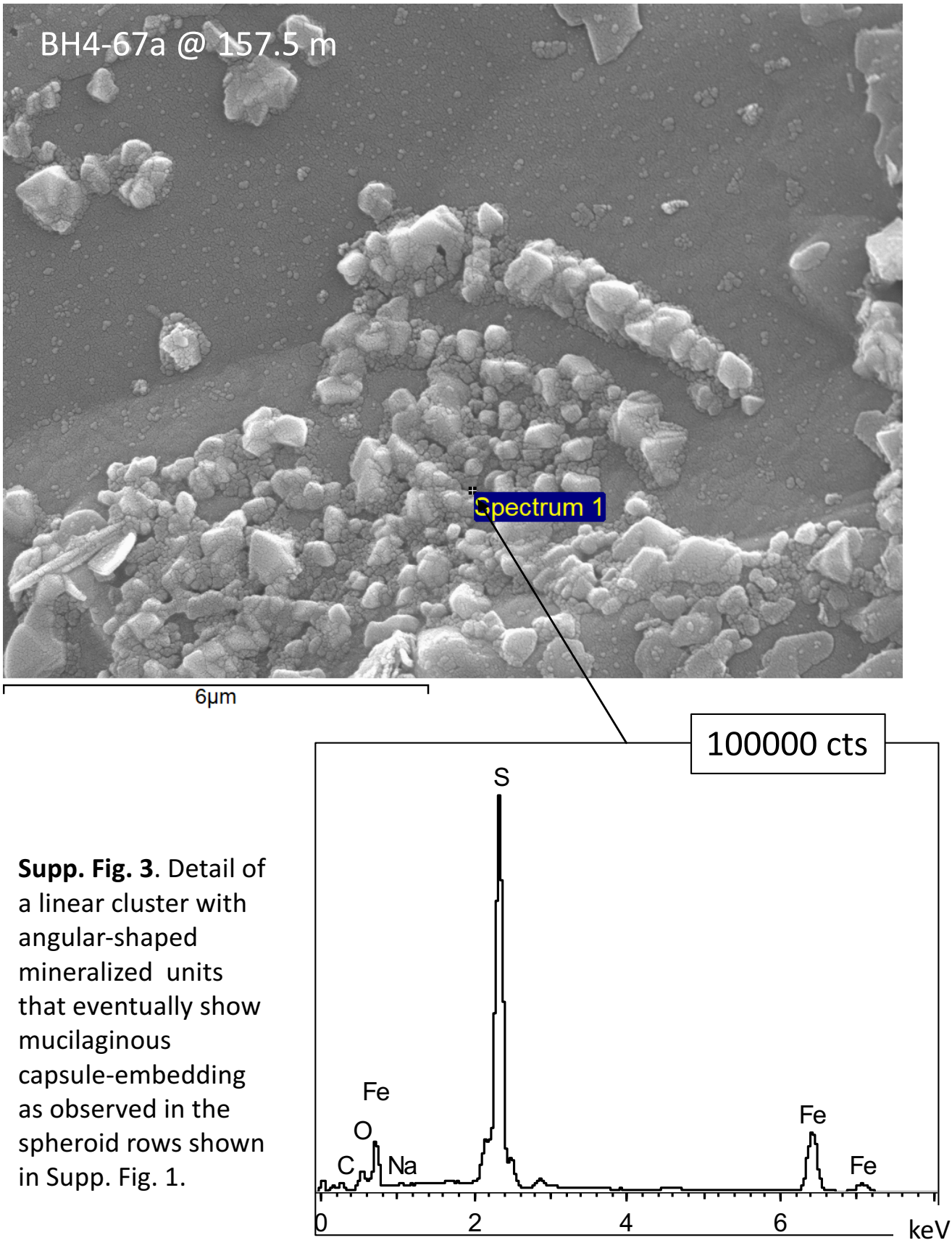

Supp. Fig. 3. Detail of a linear cluster with angular-shaped mineralized units that eventually show mucilaginous capsule-embedding as observed in the spheroid rows shown in Supp. Fig. 1.

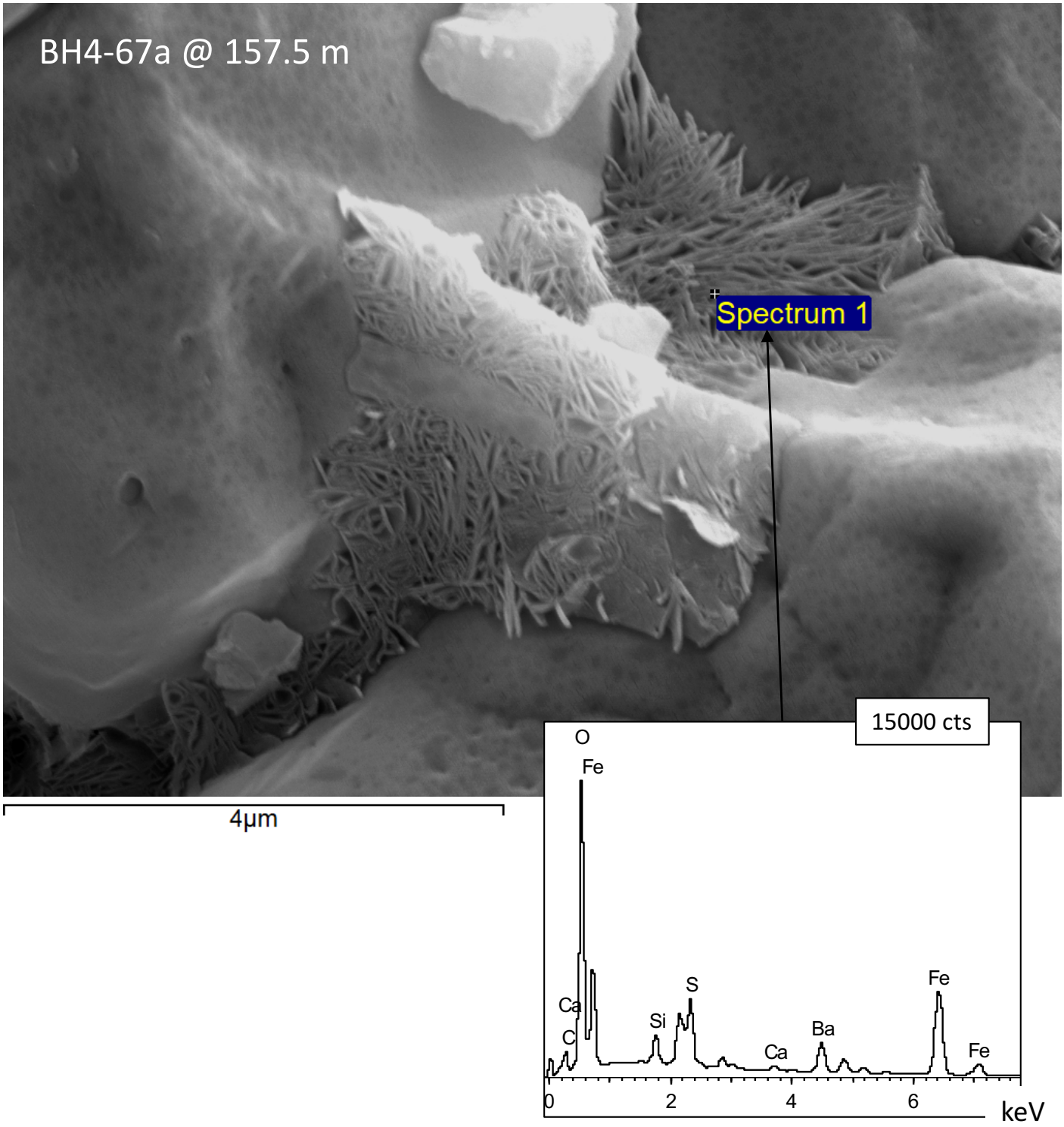

Supp. Fig. 4. EDAX spectrum of some isolated clusters of straight and bent filaments occurring on barite surface depressions which composition suggest that are the mineralized to carbonate.

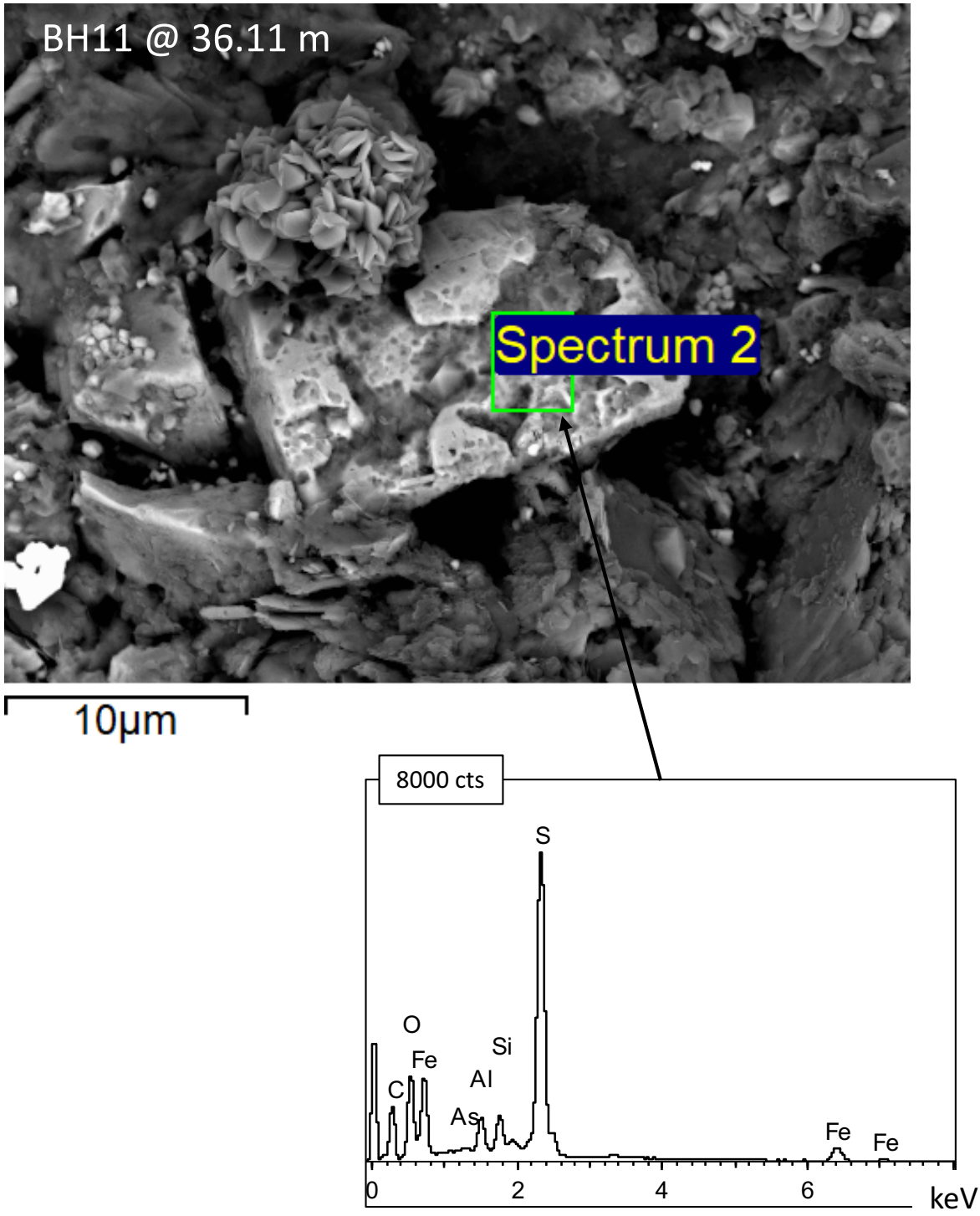

Supp. Fig. 5. Corroded surfaces affected by deep cavities that show a high C peak in the EDAX spectrum suggesting that they are filled with carbon-rich materials.

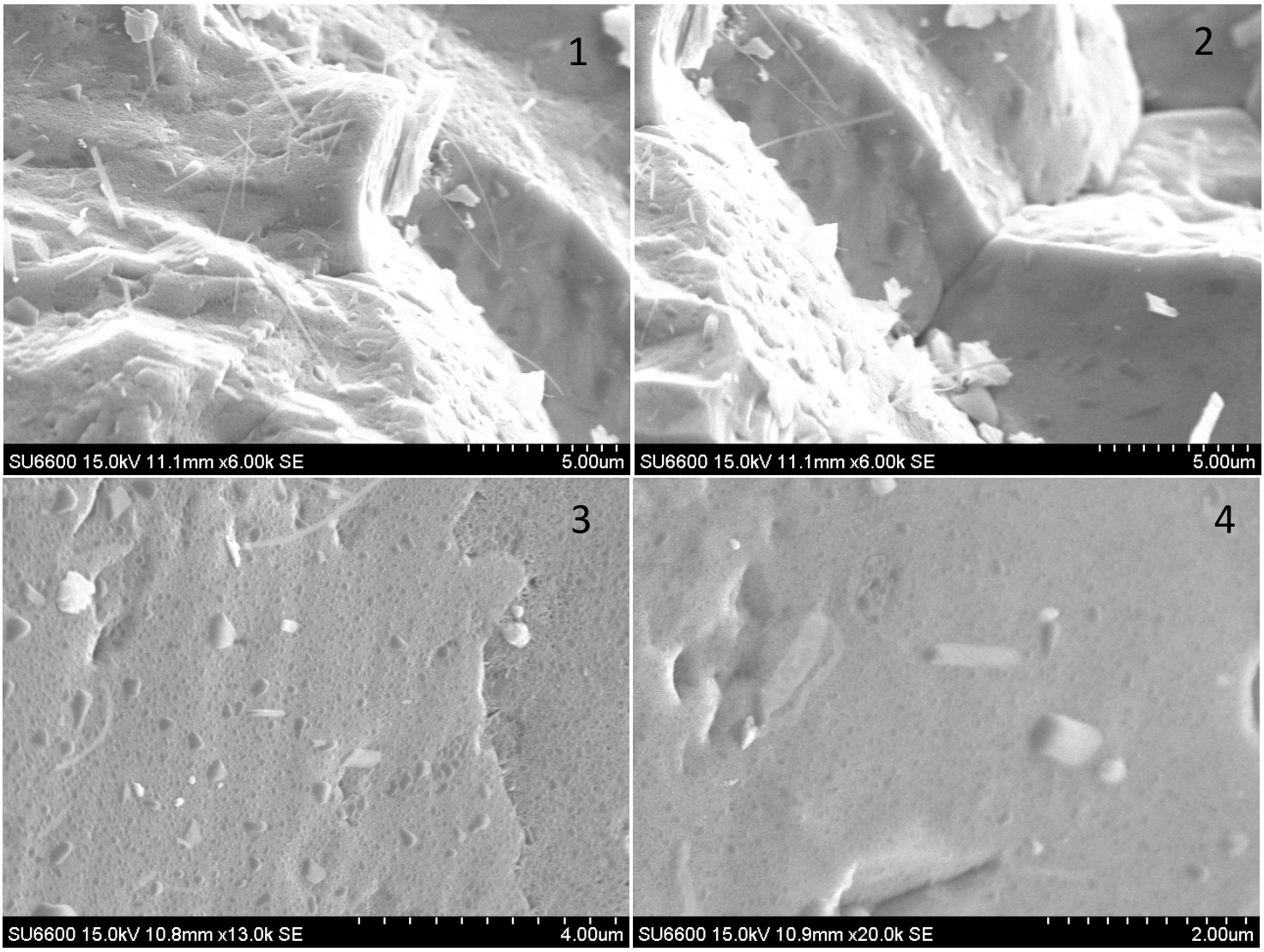

Supp. Fig. 6. Different obliteration stages **1** to **4** of the upright filaments as the SEM beam was impacting the sample surface. In stage **1**, some filaments disarranged by the SEM beam are recognized, while in stage **4** the filaments have been completely obliterated, only remaining carbonaceous

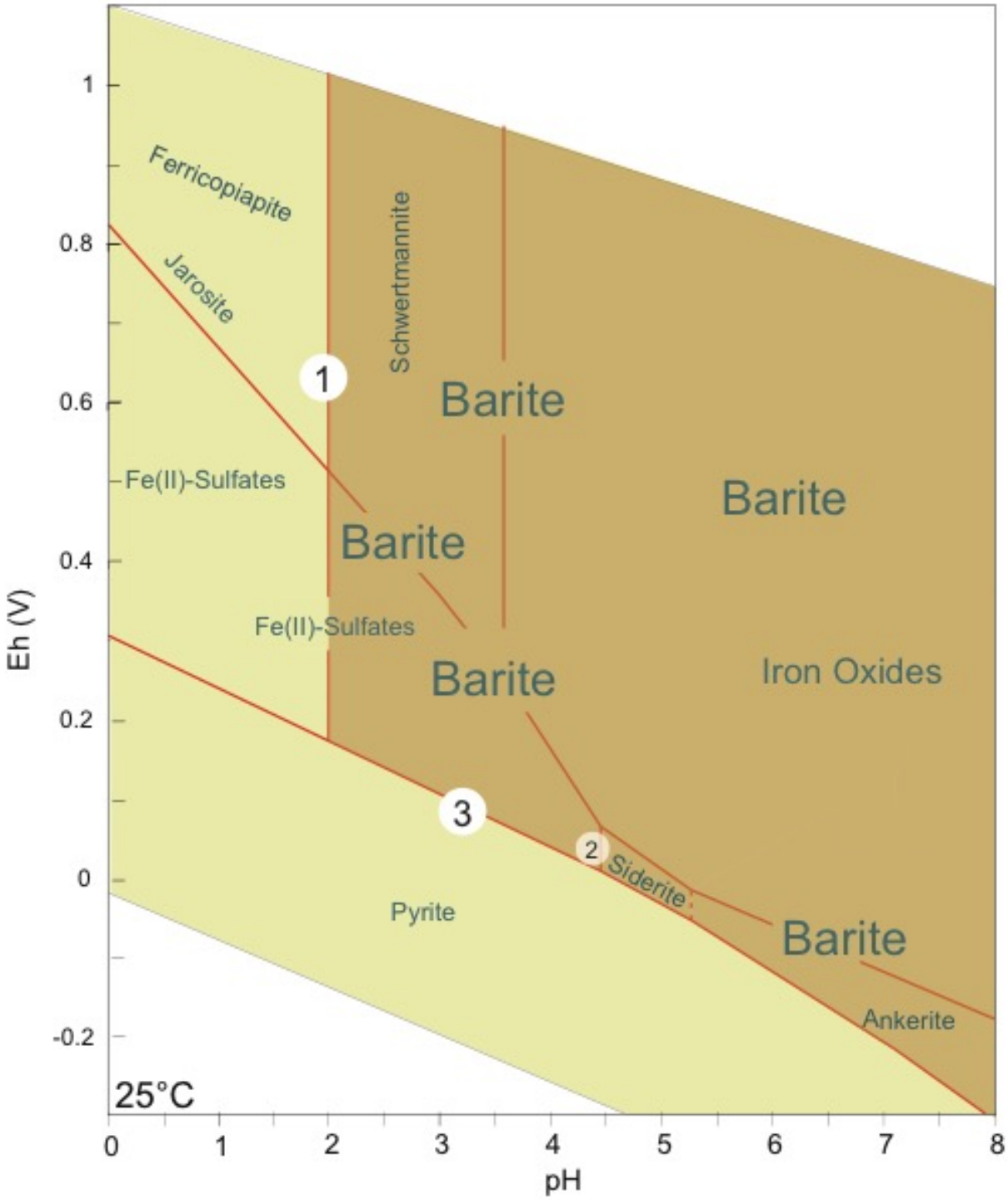

Supp. Fig. 7. pH-Eh mineral stability diagram showing the distribution of barite, pyrite and siderite/ankerite. It provides some insights in regard to the following microbial processes associated: (1) release of sulfate ions that can be driven by organic acids released by microbes, (2) bicarbonate supersaturation by sulfate reduction through the oxidation of organics, and (3) pyrite formation by sulfate and iron reduction.